



**HAL**  
open science

## Depolymerization of Technical Lignins in Supercritical Ethanol: Effects of Lignin Structure and Catalyst

Erika Bartolomei, Yann Le Brech, Roger Gadiou, Frédérique Bertaud, Sebastien Leclerc, Loïc Vidal, Jean-Marc Le Meins, Anthony Dufour

► **To cite this version:**

Erika Bartolomei, Yann Le Brech, Roger Gadiou, Frédérique Bertaud, Sebastien Leclerc, et al.. Depolymerization of Technical Lignins in Supercritical Ethanol: Effects of Lignin Structure and Catalyst. *Energy & Fuels*, 2021, 35 (21), pp.17769-17783. 10.1021/acs.energyfuels.1c02704 . hal-03469055

**HAL Id: hal-03469055**

**<https://hal.univ-lorraine.fr/hal-03469055v1>**

Submitted on 7 Dec 2021

**HAL** is a multi-disciplinary open access archive for the deposit and dissemination of scientific research documents, whether they are published or not. The documents may come from teaching and research institutions in France or abroad, or from public or private research centers.

L'archive ouverte pluridisciplinaire **HAL**, est destinée au dépôt et à la diffusion de documents scientifiques de niveau recherche, publiés ou non, émanant des établissements d'enseignement et de recherche français ou étrangers, des laboratoires publics ou privés.

# Depolymerization of technical lignins in supercritical ethanol: Effects of lignin structure and catalyst

Erika Bartolomei<sup>a</sup>, Yann Le Brech<sup>a</sup>, Roger Gadiou<sup>b</sup>, Frédérique Bertaud<sup>c</sup>, Sébastien Leclerc<sup>a</sup>, Loïc Vidal<sup>b</sup>, Jean-Marc Le Meins<sup>b</sup>, Anthony Dufour<sup>a\*</sup>

\* corresponding author : [anthony.dufour@univ-lorraine.fr](mailto:anthony.dufour@univ-lorraine.fr)

<sup>a</sup> Université de Lorraine, CNRS, Fédération J. Villermaux, Nancy, France

<sup>b</sup> Université de Haute Alsace, CNRS, IS2M, Mulhouse, France

<sup>c</sup> Centre technique du Papier, Grenoble, France

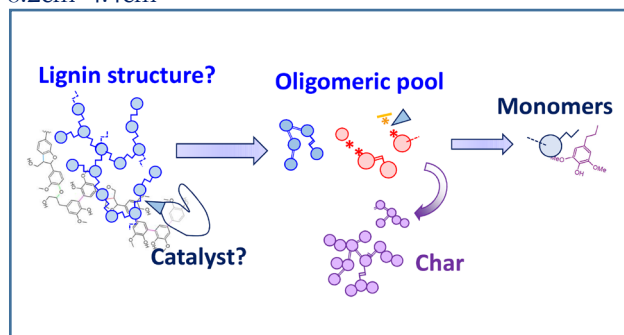
Submitted to **Energy&Fuels** for the special issue celebrating the 35<sup>th</sup> anniversary of the journal

## Table of content (only for editors and reviewers)

TOC graphic	2
Abstract	2
1. Introduction	3
2. Material and Methods	5
2.1. Characterization of the lignins	5
2.2. Characterization of the catalysts	6
2.3. Catalytic depolymerization and analysis of the products	7
3. Results	7
3.1. Characterization of lignins	7
3.2. Characterization of the catalysts	10
3.3. Effect of the catalysts on Kraft lignin depolymerization	13
3.4. Effect of technical lignin structure on their depolymerization products with Ni/C	18
4. Conclusion	22
5. Supporting information	23
6. Fundings	23
7. References	23

## TOC graphic

8.2cm\*4.4cm



## Abstract

Three complementary Kraft lignins and a Soda lignin were characterized by NMR ( $^{31}\text{P}$ ,  $^{13}\text{C}$  and HSQC) and GPC. Their theoretical yield in monomers (TMY) assuming a complete cleavage of all  $\beta$ -O-4 linkages was calculated based on these analyses. The most recalcitrant Kraft lignin based on the TMY criteria was depolymerized in supercritical ethanol (250°C,  $\text{H}_2$ , 110Bar) with Pt/C, Ni/C and Ru/C catalysts. All catalysts present an important effect on monomers (analysed by GC/MS), oligomers (by UV fluorescence) and char yields. They promote cracking reactions and the stabilization of the broken bonds by H-transfers. The hydrogenation of the side chains of the monomers is also promoted to produce notably propyl-guaiacol. We show that an oligomeric pool prevails for all catalysts. Then, the effect of lignin structure on the depolymerization mechanism was studied by comparing the 4 lignins with the less precious catalyst (Ni/C). The S/G ratio of monomers is well related to the S/G ratio of lignins. Under our conditions, the  $\beta$ -O-4 content and the TMY do not control the yields in products (monomers, oligomers or char). They are not relevant indicators for the depolymerization of these recalcitrant technical lignins. Future work should focus on novel catalysts and processes to improve the selective conversion of C-C bonds if monomers remain the targeted product.

## 1. Introduction

Lignin is the most abundant natural macromolecule composed of aromatic moieties.<sup>1</sup> Approximately 100 million tonnes of “technical lignins” are produced annually in the world.<sup>2</sup> Technical lignins are by-products of the pulping and cellulosic ethanol industries. The majority of the available technical lignins is the Kraft lignin (KL) produced in pulp mills. More than 70 millions of tonnes of KL are produced worldwide but this lignin is actually burnt in the recovery boiler of the pulp mills in order to produce steam, power and to recover pulping chemicals.<sup>3</sup> The recovery boiler is often a bottleneck to increase the productivity in pulp mills.<sup>4,5</sup> This boiler burns the black liquor (BL) which is rich in lignin. KL can be extracted from the BL in order to debottleneck the recovery boiler. For instance, the Lignoboost process extracts the KL from the BL by CO<sub>2</sub> precipitation. This process has been in operation at the industrial scale since 2013 at Domtar’s Fort Mill site in USA.<sup>6</sup>

Then, the solid lignin extracted from the BL can be valorised into bio-materials with a value over USD 1000 per tonne, compared to about USD 150 per tonne when used as a fuel. This valorisation would greatly improve the profitability of the Kraft mills.<sup>3</sup> Consequently, the global lignin market size is expected to expand. Increasing demand for lignin in animal feeds, bio-bitumen, concrete admixtures, adhesives, binders, resins (etc.) is anticipated to drive the market growth.<sup>2</sup>

Nevertheless, only a very small fraction of the worldwide KL is yet extracted and valorized for high-value chemical applications. This may be explained by the actual lower profitability of the lignin valorisation routes compared to crude oil ones<sup>3</sup> and also to the highly variable structure of KL. The chemical composition of KL depends on biomass species, seasonal and geographical location, the delignification and extraction methods. Therefore, the various available KLs exhibit a high heterogeneity in chemical functionality as well as in molecular weight.<sup>7,8</sup>

In order to tackle this high heterogeneity, it has been proposed to depolymerize lignins into monomers (like vanillin, guaiacol, phenols, benzene, etc.) or oligomers (partly depolymerized lignin). The depolymerization process reduces the molecular weight but also enables to better control the functional groups in the products (hydroxyl, methoxyl, etc.) by catalytic reactions.<sup>1,9–13</sup> The depolymerization of lignins can be conducted by pyrolysis<sup>14–19</sup>, hydrocracking/hydropyrolysis<sup>20,21</sup> or liquefaction (in the presence of a solvent such as water, alcohol, phenols, etc.)<sup>22–24</sup>. The mechanisms of lignin depolymerization have been extensively reviewed.<sup>9,11,13</sup>

The KL exhibits a more recalcitrant structure than the native lignin present in biomasses impeding its depolymerization.<sup>11,13,25,26</sup> Indeed, the Kraft pulping involves fragmentation and repolymerization reactions leading to a recalcitrant and condensed lignin with a low content in ether bonds.<sup>7</sup> For this reason, Xu et al. have proposed to produce a partly depolymerized KL (D-KL) instead of monomers.<sup>3,27</sup> D-KL could be a better target than monomeric phenols and a profitable bio-substitute to petroleum-based polyols to produce polyurethane foams or phenolic resins.<sup>3</sup> Recently, depolymerized lignin oils have been produced at pilot scale replacing up to 67% of bisphenol A to produce a cured epoxy polymers with improved properties.<sup>28</sup>

Catalytic reductive depolymerization of lignin has appeared to be a promising method to promote the formation of phenolic compounds. It is often performed in the presence of metallic nanoparticles (Ru, Ni, Pd, Pt, Fe, Cu, etc.) supported on a porous material (Al<sub>2</sub>O<sub>3</sub>, TiO<sub>2</sub>, activated carbons, etc.)<sup>29–34</sup>, a reducing agent (mainly hydrogen) and a solvent.<sup>13,35</sup> Reductive depolymerization promotes the formation of low

molecular weight phenols by stabilizing the cleaved bonds by H-transfers. Molecular hydrogen can be brought by H<sub>2</sub> or by organic H-donors.

Supercritical alcohols are promising solvent for lignin depolymerization because of their high heat transfer, high solubilisation capability, and good H-donor behavior<sup>29,31,36</sup>. Ethanol is a cheap and green alcohol of high interest for lignin liquefaction<sup>37</sup>. It reduces the repolymerization of lignin decomposition products<sup>31</sup>.

An overview of the published work on technical lignins depolymerization in supercritical alcohols is presented in supporting material (table S1).

Most of the time, harsh conditions were tested, namely: temperature higher than 300°C leading to high pressures (higher than 200 Bars) required to maintain the alcohol at the supercritical state.

These studies have shown the interest of using supercritical ethanol combined with a metal catalyst to produce phenolic species but they did not explore milder conditions of potential interest for the industrial deployment of this technology in Kraft mills. Indeed, reactor pressures not higher than about 150 Bars may be rather targeted.<sup>23,38</sup>

Previous studies have also shown the potential of catalysts based on metals (Ru, Ni, Pt) deposited on carbonaceous supports. Activated carbons are relatively stable supports under the liquefaction conditions.<sup>39</sup> For these reasons, this present work compares commercial Ru, Ni and Pt catalysts supported over activated carbons. These catalysts were not yet compared for a Kraft lignin under mild supercritical ethanol conditions (250°C, 100 Bar). Their deactivation was not yet assessed under such conditions.

Despite the numerous studies on lignin depolymerization, we did not find articles dealing with the effect of the structure of different Kraft lignins under supercritical ethanol conditions. This topic is of high importance considering the heterogeneous structure of industrially available KL.

Different technical lignins were compared under other depolymerization conditions than supercritical ethanol. For instance, Kraft, Organosolv and Soda lignins were compared by De Wild et al. in a 2 stage process including pyrolysis and the hydrodeoxygenation of the bio-oils.<sup>40</sup> They showed an important impact of the lignin type on the composition of monomers and that a direct hydrotreatment of lignin gives a higher monomers yield than the 2-stage process. The effect of the type of lignins (hardwood, softwood, Kraft, Soda, Organosolv, etc.) was highlighted by Cabral Almada et al. in a basic solution and without catalyst for oxidative (air) depolymerization.<sup>41</sup> They have demonstrated a relation between the accessible phenol moieties, inter-unit linkages and the yields in aromatic compounds. Phongpreecha et al.<sup>42</sup> have related the monomer yields (after hydrogenolysis with Ni/C catalyst) for different alkali lignins as a function of their  $\beta$ -O-4 content. Amiri et al.<sup>43</sup> have completed the approach of Phongpreecha et al.<sup>42</sup> by using a simple ether cleavage model to predict the final depolymerization yields in monomers. Recently, Xiao et al.<sup>44</sup> have studied the effect of diverse lignins prepared from Eucalyptus with varying  $\beta$ -O-4 contents (on a large range) and phenolic hydroxyl groups. They clearly show a relation between monomers yields and  $\beta$ -O-4 contents. The Kraft lignin produces less than 5wt.% monomers under their conditions (Pd/C, methanol, H<sub>2</sub>, 180°C, 4h). Bouxin et al.<sup>45</sup> have prepared uncondensed lignins (by ammonia mild pretreatment) and more condensed ones by Soda and organosolv pulping from the same biomass (poplar). The lignins were depolymerized by Pt/Al<sub>2</sub>O<sub>3</sub> under H<sub>2</sub>, methanol/water mix, at 300°C during 2h. These authors have also shown that the content in  $\beta$ -O-4 bonds is a crucial factor for the production of monomers.

All these studies have compared lignins with relatively high  $\beta$ -O-4 contents or presenting a large range of  $\beta$ -O-4 contents. They did not compare different Kraft lignins.

Despite all these extensive studies and to the best of our knowledge, the effect of the structure of technical lignins on their depolymerization products is still poorly understood and notably under mild

supercritical ethanol. For instance, it remains unclear if their low content in  $\beta$ -O-4 linkages controls the monomer yields.

For this reason, we have selected relevant industrial lignins and characterized their structure by NMR methods. We compare their depolymerization behaviours and relate the produced monomers to their chemical structure.

To sum-up, the novelty of this work lies on the 3 following aspects:

- 1) Ni, Ru, Pt/C catalysts are compared and their deactivation is assessed;
- 2) 4 relevant and complementary technical lignins are characterized;
- 3) The relations between the lignins' structure and their depolymerization products are discussed.

## 2. Material and Methods

The global methodology of this work is presented in Figure 1.

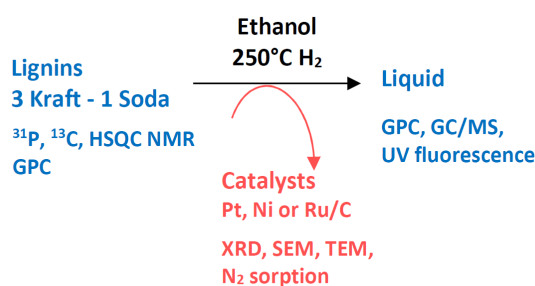


Figure 1. Analytical methods used in this work

First, the lignins were characterized by NMR ( $^{13}\text{C}$ ,  $^{31}\text{P}$  and HSQC-heteronuclear single quantum coherence) and GPC. They were converted at  $250^\circ\text{C}$ , in supercritical ethanol and with catalysts. The catalysts were characterized before and after reaction by Scanning and Transmission Electron Microscopy (SEM & TEM), XRD and  $\text{N}_2$  sorption. The liquid products were analyzed by UV fluorescence, GPC and GC/MS. We have justified in our previous article<sup>46</sup> the interest of UV fluorescence as a fast method to assess the distribution in monomers and oligomers produced by lignin depolymerization. The analytical methods were developed under different conditions (Soda lignin, Pt/C catalyst)<sup>46</sup> than the ones presented in this work.

### 2.1. Characterization of the lignins

The lignins studied in this work are presented in table 1. These lignins were selected as the most representative and available technical lignins. It is of high importance to compare the depolymerization of these industrial lignins in order to assess the feasibility of lignin depolymerization integrated in the existing pulp mills.

Table 1. Code and suppliers of the selected technical lignins

Code name	Lignin type	Biomass	Supplier
K1	Kraft - LignoBoost "BioPiva 100"	Southern Pine wood	UPM Biochemicals (Finland), produced by DOMTAR Plymouth, USA (Biochoice process)
K2	Kraft	Eucalyptus	Fibria produced on a pilot at 500t/year in the mill of Jacarei (Brazil)
K3	Kraft – pilot stage, produced by the authors	Pine wood	Black liquors sampled, in the frame of this present work, at the Fature pulp plant (Smurfit Kappa, France), mainly using Pinus Pinaster wood, and then lignin precipitated by CO <sub>2</sub> for this study (see supporting material for the protocol)
Soda	Soda lignin - Protobind 1000	Wheat straw	Green Value (USA), produced in India

The K3 lignin has been tailor produced from a BL sampled in an industrial Kraft mill for this work (see supporting material for the complete procedure). The 3 other lignins have been provided by the suppliers. NMR (<sup>31</sup>P NMR, <sup>13</sup>C and HSQC) and GPC methods are described in supporting material.

## 2.2. Characterization of the catalysts

3 catalysts were selected based on the literature review. 5wt.% Ru/C and 5wt.% Ni/C were supplied by Ryogen (ref.0139-CRuA05 and 0158-CNiA05 respectively), 5 wt.% Pt/C by Sigma Aldrich (ref. 908010).

The morphology of the catalysts before and after reaction was characterized by Scanning Electron Microscopy (SEM) on a JEOL JSM-6490LV microscope combined with energy dispersive X-ray spectroscopy (EDX) for analysing the global composition of the particles.

Transmission Electron Microscopy (TEM) images of the catalysts were obtained with a JEOL ARM200-CFEG microscope operating at 200 kV. The catalyst powders were dispersed into chloroform by ultrasonic treatment and the obtained suspensions were deposited on a gold observation grid covered with a film of an amorphous carbon. The particle size distribution of metallic nanoparticles was obtained by analysing the TEM images. 50 to 100 particles were detected and their size was computed from the projected area of each particle (under the ImageJ software).

The textural properties of the catalysts before and after reaction were obtained from adsorption isotherms of N<sub>2</sub> at 77K. The experiments were done on a Micromeritics ASAP 2420 device in the relative pressure range 10<sup>-7</sup> - 1. Prior to the analysis, the samples were outgassed at 300°C during 12 hr. The CO<sub>2</sub> adsorption isotherms at 273K were measured on the same experimental set-up. The surface area of the materials was obtained by applying the BET equation in the relative pressure range 0.01 - 0.05 since most samples exhibited significant amount of micropores. The total pore volume was calculated from the N<sub>2</sub> volume adsorbed at a relative pressure of 0.99. The volumes of micropores (pore diameter below 2nm) and of narrow micropores (i.e. ultramicropores with a diameter below 0.7 nm) were obtained by applying

the Dubinin-Radushkevich equation on the N<sub>2</sub> and CO<sub>2</sub> adsorption isotherms, respectively. Pore size distribution was obtained by using the NL-DFT model for slit pores with finite depth.

The structure of the catalysts was analyzed by X-ray diffraction (XRD) with a Bruker D8 Advance X-ray diffractometer. The detector was a LYNXEYE XE-T 1-D detector in high resolution mode fully opened (2.72°). The wave length used was CuK $\alpha$ 1,2. The diffractograms were recorded for 2 $\theta$  angles between 10° and 130° at a step scan of 0.014° with a step time of 1.80 s. The diffractometer used fixed divergence slits (0.03°). An automatic motorized anti-scatter screen was used to avoid air-scattering at low angles.

### **2.3. Catalytic depolymerization and analysis of the products**

The methods for the liquefaction and analysis of liquids were previously presented in our previous article.<sup>46</sup> Briefly, lignin depolymerization was carried out in a 300 mL autoclave. The reactor was loaded with 10 g of lignin, 200 mL of pure ethanol and Pt/C, Ru/C or Ni/C catalyst to reach 1% wt., metal load based on lignin mass (2.0 g of Met/C catalyst, 5% wt. of metal loading, leading to 0.1g of metal for 10g lignin). 100  $\mu$ l of hexadecane was injected as an internal standard (with the 200mL ethanol, lignin and catalyst) for a more accurate quantification of monomers by GC/MS-FID. The autoclave (stirred at 400 rpm) was purged several times, then charged with 10 Bar H<sub>2</sub> and heated up to 250°C at 5 K/min, and maintained during 4h at 250°C. The final pressure was 110 Bar. The liquid was sampled under isothermal condition (at 250°C) at different time on stream as previously presented.<sup>46</sup> The time “0” is defined once the temperature reached 250°C (first sampling).

The catalysts and solid particles were recovered by filtration (at 1.2 $\mu$ m) of the whole remaining solution after the 4 hours of reaction. Char yield was calculated by subtracting the mass of catalyst.

The sampled liquids were analyzed by:

- 1) GPC-UV (in THF without acetylation);
- 2) GC/MS-FID by the internal calibration method;
- 3) UV fluorescence with 20nm offset as justified in our previous work<sup>46</sup>.

The analytical methods are presented in supporting material.

## **3. Results**

### **3.1. Characterization of lignins**

The chemical composition of the 4 lignins is presented in table 2.

Table 2. Main chemical properties of the 4 technical lignins

Chemical properties	Lignin K1	K2	K3	Soda	Method
Mw (Da)	7600	4300	8600	4200	GPC
CHO	65.5/5.6/21.1	63.6/5.3/26.4	71/5.6/21.3	64.6/5.6/25.5	(wt.%) Elemental analysis
NS	<0.1/2.1	0.1/2.4	<0.1/2.0	0.5/0.7	
Na	0.16	0.17	0.28	0.09	(wt.%) ICP-OES <sup>47</sup>
K	0.01	0.04	0.15	0.04	
C=O Ester mainly acetate (185 – 167ppm)	2.4	0.9	3.4	2.3	<sup>13</sup> C NMR (mmol/g lignin)
Aromatic C-O (164 – 140ppm)	14.3	12.4	12	11.5	
Aromatic C-C (140 – 100ppm)	22.5	24.5	19.4	23.5	
Aliphatic C-O (100 – 60ppm)	5.6	4.8	8.9	4.8	
Methoxyl (60-51ppm)	5.4	8.4	4.6	6.7	
Aliphatic (35-10ppm)	4.4	2.1	10.9	5.1	
Ali-OH (150-145ppm)	1.66	1.39	1.28	1.32	<sup>31</sup> P NMR (mmol/g lignin)
Syringyl OH/ Condensed structure (144-140ppm)	1.9	3.45	1.21	2.3	
Guaiacyl OH / p-hydroxy phenyl OH (140 - 136 ppm)	2.91	1.38	1.74	1.64	
Carboxylic acid (136-132 ppm)	0.58	0.48	0.4	0.9	
%G	96.9	26.9	98	42.5	HSQC NMR (mol. %), S+G+H = 100%
%S	0	73.1	1	54.3	
%H	3.1	0	1	3.2	
β-O-4	7.6	9.1	4.8	5.5	HSQC (number of linkages per 100 aromatic rings)
β-β	4.4	6.4	4.8	4.1	
β-5	3.2	0.7	2.5	1.2	
Empirical formula of a C <sub>9</sub> based monomer	C <sub>9</sub> H <sub>7.5</sub> O <sub>1.5</sub> (OCH <sub>3</sub> ) <sub>0.88</sub>	C <sub>9</sub> H <sub>6.3</sub> O <sub>1.9</sub> (OCH <sub>3</sub> ) <sub>1.37</sub>	C <sub>9</sub> H <sub>6.7</sub> O <sub>1.3</sub> (OCH <sub>3</sub> ) <sub>0.88</sub>	C <sub>9</sub> H <sub>7.1</sub> O <sub>1.9</sub> (OCH <sub>3</sub> ) <sub>1.15</sub>	Calculated based on the GPC, NMR and elemental analysis and on ref. <sup>26,43</sup>
Degree of polymerization (D.P.)	13.0	6.6	15.0	6.7	
Fraction of cleavable bonds (F <sub>CB</sub> ) (%)	8.2	10.7	5.1	6.5	
Theoretical yield in monomers (TMY) assuming complete cleavage of β-O-4 (%)	1.8	4.1	0.9	2.2	

The molecular weights of K2 and Soda lignins (~4000 Da) are lower than the ones of K1 and K3 (7600 and 8600 Da). These molecular weights are usual values for technical lignins<sup>26,48</sup>.

K1, K2 and soda lignins present a similar carbon content (65%wt.). K1 and K3 have a lower oxygen content. The sulphur content is similar in the 3 Kraft lignins (about 2 wt.%) but lower in the Soda lignin. The Soda lignin has a higher N content.

The main linkages present in the technical lignins are displayed in figure 2.

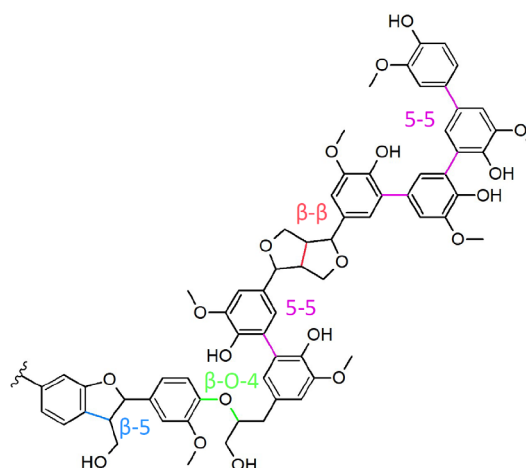


Figure 2. Simplified structure of a segment of the technical lignins, representing some important moieties as analyzed by NMR

This simplified scheme does not depict the distribution of all the moieties in relation to their NMR quantification. It is presented to support the discussion and to illustrate the diversity of moieties in the technical lignins. More advanced structures were proposed for Kraft and Soda lignins<sup>7,9,48</sup>. This scheme only presents a segment of lignin molecules. Indeed, our technical lignins present an average degree of polymerization (DP) between 6 and 15 of C<sub>9</sub> aromatic units (see table 2). The DP of K2 and Soda lignins is lower and of about 6 aromatic units. The content in  $\beta$ -O-4 bonds is lower than 10 linkages per 100 aromatics units (table 2) for all the lignins, which is in agreement with previous studies<sup>7,26,48</sup>. The K2 lignin presents the highest content in  $\beta$ -O-4 and  $\beta$ -5 linkages. It has the highest content in syringyl and methoxyl groups because this lignin is produced from Eucalyptus (see tables 1 and 2). K1 lignin is the richest lignin in guaiacyl groups.

The fraction of cleavable bonds ( $F_{CB}$ ) and the theoretical yields in monomers (TMY) are presented in table 2. They are based on the approach proposed in previous work<sup>26,43</sup> and on our present analyses. It has been previously shown in several studies that the monomer yields under solvent depolymerization conditions can be related to the content in  $\beta$ -O-4 bonds<sup>42-45</sup>. Therefore, it is of interest to calculate a theoretical yield in monomers by assuming a complete conversion of the  $\beta$ -O-4 bonds<sup>26,43</sup> in order to compare the theoretical potential of our lignins. TMY increases for lower DP lignins and higher  $\beta$ -O-4 contents.

Our results are in very close agreement with a recent characterization of similar technical lignins.<sup>26</sup> TMY ranges between 0.9 to 4.1% for our 4 lignins with K3 being the most recalcitrant lignin (based on this theoretical calculation) due to its higher molecular weight and lower content in  $\beta$ -O-4 bonds. These very low TMYs infer that all our technical lignins would yield to very low monomer yields if we assume the complete cleavage of the  $\beta$ -O-4 bonds. This outcome is further discussed in the next sections and is related to the analysis of liquid products obtained after catalytic depolymerization.

### 3.2. Characterization of the catalysts

First, the most recalcitrant lignin (K3, based on TMY calculation) was tested on the 3 catalysts. The catalysts were characterized by SEM-EDX before and after K3 lignin depolymerization (figure 3).

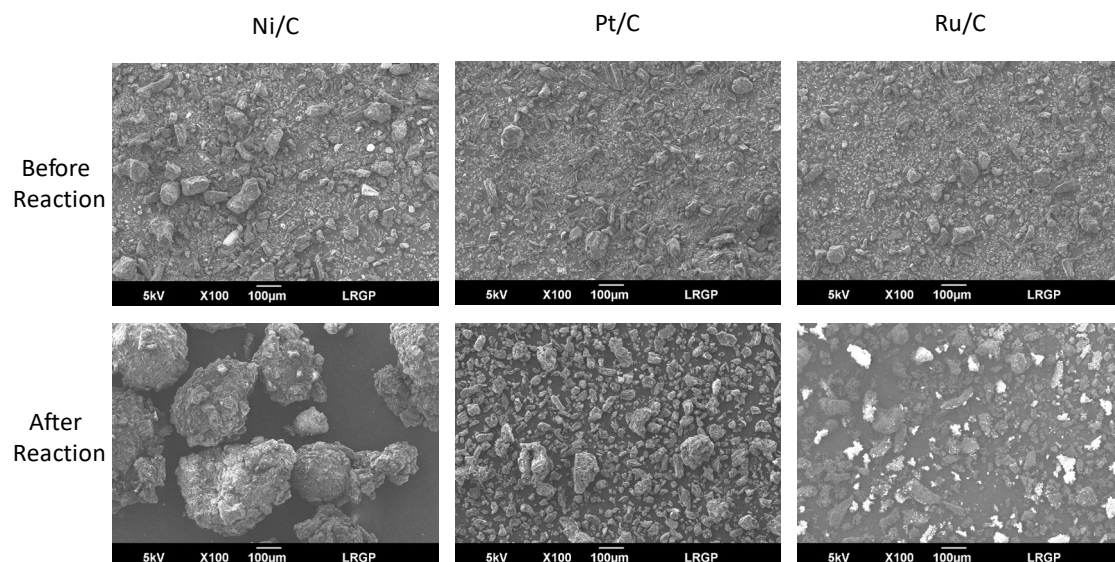


Figure 3. SEM analysis of the catalyst before and after K3 lignin depolymerization (4h, 250°C, ethanol)

The EDX mappings of the main elements (C, O, Si, metal, S, etc.) are presented in supporting information.

The catalysts present a large range of particle sizes between about 10 and 100 μm. After reaction, bigger particles are formed notably for Ni/C catalyst, highlighting an agglomeration of catalyst particles by lignin-based softened and sticky intermediates<sup>49</sup>.

The EDX analysis (figure S7 in supporting material) clearly displays a decrease in metal content after the reaction on the surface of all catalyst particles and a relatively homogeneous composition (at the μm scale) of the deposit which is mainly composed of C, O, Na, S. Because our catalysts are composed of carbon as the support of metals, sulphur and sodium are good indicators of the origin of the carbon deposit coming from lignin intermediates (2 wt.% of S in K3 lignin, table 2). The oxygen content of the deposit is also higher than the one of the support. Bright particles for Ru/C after reaction are due to contrast analysis issues. We checked by EDX that the composition of the brighter particles was similar than the other ones (mainly based of C, O and S from lignin deposit).

The ratio of S/metal element (or O/metal) may be used as a broad indicator of the lignin-based deposit over the particles of catalysts. Pt/C and Ru/C present a lower ratio and especially Pt/C is less recovered by lignin-based deposit with still an important fraction of Pt detected by EDX after reaction (figure S7). To the best of our knowledge, this deposit of lignin-based material over catalysts had yet been poorly evidenced. It is sometimes leached by solvents before catalyst recycling tests<sup>50</sup>.

At a smaller scale of observation, TEM highlights the global atomic structure of the carbon support (figure 4) and the size of the nanoparticles of metals.

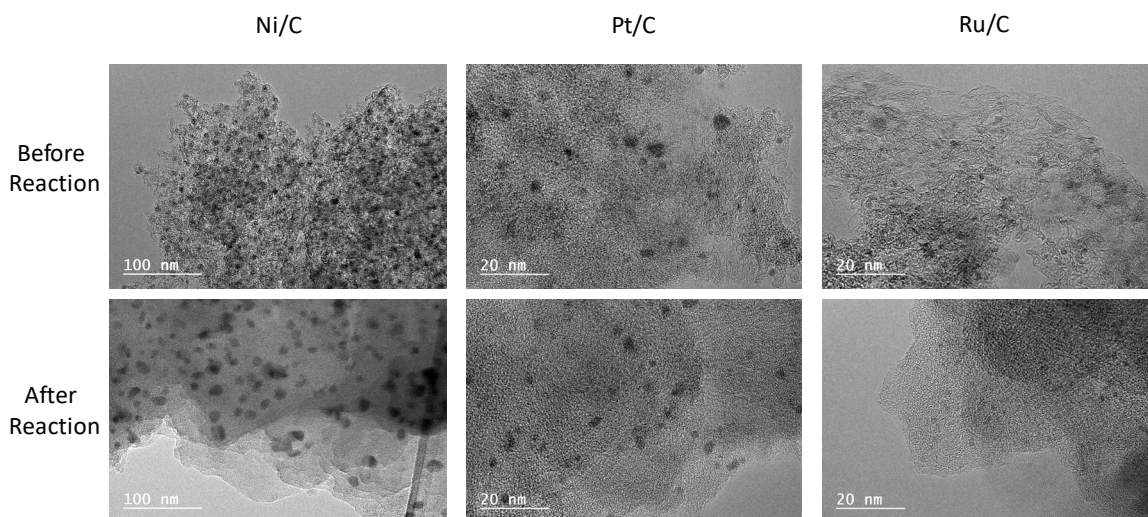


Figure 4. TEM analysis before and after K3 lignin depolymerization

The carbon support is mainly composed of microporous disordered carbons which is typical of activated carbons produced from the pyrolysis of biomass. It was not possible to discriminate by TEM the deposited carbon after reaction vs. the carbon of the support. Further analysis would be needed to identify the structure of the lignin-based carbon deposit, for instance by solvent extraction, advanced NMR, differential thermal annealing<sup>51</sup> or XPS.

The particle size of the metallic nanoparticles has been analyzed by TEM and is given in supplementary material (figure S8). Before K3 depolymerization, the average nanoparticle size is 9.1nm, 2.6nm, 2.1nm for Ni, Pt and Ru respectively. The metals and notably Pt and Ru are well dispersed in these catalysts.

Nickel mean particles size increases from 9.1 to 12.1 nm after reaction. Platinum and ruthenium catalysts are less impacted by the reaction.

Metallic nanoparticles dispersed on a carbon support exhibit different mobilities, which depend on the nature of the metal and on the temperature<sup>52</sup>. For a given metal, this mobility is correlated with the so-called “Tammann temperature”, defined as 50% of the fusion temperature<sup>53</sup>. The growth of the nanoparticles during catalytic reactions is strongly related to this mobility. For the three metals tested here, the Tammann temperatures are 863, 1020 and 1291 K for Ni, Pt and Ru, respectively. These values shows that the mobility of nickel nanoparticles is higher than the one of Pt and Ru nanoparticles in carbons. Due to their higher Tammann temperature, platinum and ruthenium nanoparticles are more stable.

A second mechanism known as Ostwald ripening can lead to the sintering of nanoparticles<sup>54</sup>. It is based on dissolution-migration-recondensation which might occur on the metallic phase during the catalytic depolymerization. The dissolution step of Ostwald ripening strongly depends on the different reactions which can take place and the migration step can occur through the fluid phase (3D mechanism) or on the catalyst surface (2D mechanism)<sup>55</sup>. It remains unclear which detailed mechanism can explain the increase in particle size of Ni/C under supercritical ethanol conditions.

Then, the composition of the crystals was studied by XRD. XRD diffractograms of pristine and spent catalysts are presented in supporting material (figure S9). Metallic nanoparticles can be detected by the peaks at 44.55 and 51.91° for Ni, 39.76 and 46.24° for Pt, 44.10 and 42.18° for Ru. It was not possible to use the Scherrer equation to calculate a mean crystal size because the amount of the metal was too low (as shown by EDX for Ni catalyst) or the particle size was too small (as shown by TEM analysis for Ru and Pt catalysts). SEM-EDX analysis shows that Ru-C and Ni-C catalysts have a significant silica content. This

is confirmed by XRD analysis which evidences the presence of silica crystals (main peaks at 20.86, 26.64 and 68.2°). These peaks are lowered after reaction maybe due to a partial dissolution of silica in supercritical ethanol.

After reaction, several new peaks can be observed and the diffractograms are more difficult to analyze. Some peaks are related to sodium sulfate deposits with main peaks at 22.54 and 31.19 and 33.11° (PDF 27-0791). This is in agreement with the significant content of sulphur and sodium observed by EDX in the spent catalysts coming from the lignin-based deposit. We did not detect the presence of sulfided metals. A sulfidation of the metallic phase does not seem the major mechanism of deactivation of the catalyst under our conditions, despite the high content in sulfur of K3 lignin.

The textural properties of the pristine and spent catalysts are presented in Table 3.

Table 3. Total pore volume ( $V_p$ ), BET surface area ( $S_{BET}$ ), micropore volume ( $V_{N_2}$ ) and ultramicropore volume ( $V_{CO_2}$ ) for pristine and spent catalysts after K3 lignin depolymerization

	$V_p$ (cm <sup>3</sup> /g)	$S_{BET}$ (m <sup>2</sup> /g)	$V_{N_2}$ (cm <sup>3</sup> /g)	$V_{CO_2}$ (cm <sup>3</sup> /g)
Pt/C-BR (before reaction)	1.29	1541	0.52	0.25
Pt/C-AR (after reaction)	0.17	103	0.04	-
Ru/C-BR	0.68	757	0.30	0.21
Ru/C-AR	0.01	7	0.00	-
Ni/C-BR	0.64	910	0.34	0.24
Ni/C-AR	0.02	16	0.00	-

The nitrogen adsorption isotherms are provided in supplementary material (figure S10). Before reaction, the three catalysts have significant high surface areas. Pt/C-BR (before reaction) exhibits a large micropore volume (0.52 cm<sup>3</sup>/g). The mesopore volume estimated from the difference  $V_p - V_{N_2}$  is also high (0.77 cm<sup>3</sup>/g). This material is typical of highly activated carbons. The Ru and Ni based catalysts have a lower surface area, with a lower micropore volume and also a lower mesopore volume. It must be noticed that the three catalysts have a very similar volume of ultramicropores which is obtained from CO<sub>2</sub> adsorption isotherm. This is typical of carbon materials with a very low level of organisation.

After K3 lignin depolymerization, the surface areas and porosities of the 3 catalysts are strongly decreased. In the case of ruthenium and nickel catalysts, the materials are even no more porous. Pt/C-AR keeps a surface area of 103 m<sup>2</sup>/g after reaction (table 3). Its micropore volume has decreased to a very low (but not null) value and, contrary to the two other catalysts, some small mesopores (5-10nm) are still observed in the platinum catalyst. The distribution of pore sizes as determined by NL-DFT is presented in supplementary material (figure S11). It clearly shows the plugging of the majority of pores with a lower plugging of pores (> 5nm) for Pt/C catalyst. This result is consistent with a lower deposit of lignin-based carbon over Pt/C as detected by SEM-EDX.

### 3.3. Effect of the catalysts on Kraft lignin depolymerization

The 3 catalysts (Ni/C, Ru/C, Pt/C) were compared on K3 lignin, the most recalcitrant one based on TMY calculation.

Table 4. Yields of char and monomers (by GC/MS) after 4 hours of reaction at 250°C for K3 lignin

Catalyst	no catalyst	1% Ru	1% Ni	1% Pt
Char (%wt)	46.7	22.5	27.7	15.0
Monomers (%wt)	2.4	4.1	4.7	5.1

Table 4 shows that the char yields are importantly decreased by the 3 catalysts and especially for the Pt/C catalyst, in good agreement with Kim et al.<sup>29</sup>. These authors also found that Pt/C produces less char than Ru and Ni/C but under more severe conditions than ours (350°C, ethanol). Pt/C promotes the transfer of H atoms (from ethanol) and the subsequent stabilization of the broken reactive bonds.<sup>46,56</sup> It reduces secondary condensation reactions leading to char.

The 3 catalysts also promote the stabilization of monomers by H-transfer reactions. Indeed, the monomer yields as determined by GC/MS is about doubled by the 3 catalysts compared to the uncatalyzed test, but these yields (of about 5 wt.%) are still low due to the relatively mild conditions selected in this work (250°C, 110 Bar) and to the high recalcitrance of the Kraft lignin.

The liquid products present a similar molecular weight of about 800 Da for all conditions (by GPC, table S5). It means that lignin is depolymerized to produce mainly oligomers in the range of 3-5 aromatic units (~800 Da). This result is again in excellent agreement with Kim et al.<sup>29</sup>. It confirms our proposed mechanism<sup>46</sup> highlighting that an “oligomeric pool” prevails upon the depolymerization of lignin. In this present work, we show that this oligomeric pool occurs whatever the catalyst used. The 3 catalysts present mainly micropores with important diffusion limitations for the transfer of lignin and oligomers. Therefore, lignin and oligomers conversion are likely to occur at liquid state or on the external surface of the catalyst as it is highlighted by the deposit of the lignin-based material over the catalysts (analyzed by SEM-EDX).

The importance of this oligomeric pool is also well depicted by the UV fluorescence analysis of the liquids. Lignin produces a continuum of molecules from oligomers to monomers. It is of high importance to analyze this continuum of molecules for understanding the mechanisms of lignin depolymerization. We have previously demonstrated that UV fluorescence is an interesting technique to assess fastly this continuum without samples' pre-treatment<sup>46</sup>. The emission peak of UV fluorescence is related to the number of undisrupted conjugated bonds in molecules and, therefore, to the molecular weight of the conjugated molecules.<sup>57-59</sup> UV fluorescence is a relevant technique in our case because our technical lignins (table 2) and the depolymerization products are mainly composed of conjugated moieties, but it is only semi-quantitative owing to the complexity of the molecular pool. The UV fluorescence spectra are presented in supporting material (figure S12). They depict 3 main peaks as previously unraveled<sup>46</sup>: at around 375nm (lignin), 350nm (oligomers), 305nm (monomers). They show a progressive decrease of the lignin peak accompanied with an increase in oligomers and monomers peaks upon the conversion time. For all conditions, the peak at 375nm is the major one up to the first 30 minutes. Then the peak of oligomers dominates the signal after 2 hours of conversion time for Pt/C. Ni/C presents a slower decrease of the lignin peak than Ru and Pt/C which is consistent with the known higher reactivity of Pt

and Ru for cracking reactions compared to Ni.<sup>60</sup> The importance of the oligomer peak at a constant emission wavelength (350 nm) confirms the results of the GPC analysis that an oligomeric pool dominates the continuum of molecules and that its molecular weight (related to the emission wavelength) stays globally constant for all conditions. In this oligomeric pool, a competition between depolymerization (bonds breaking) and reoligomerization (or condensation) reactions may occur. Possible condensation reactions of lignin fragments were reviewed recently.<sup>61</sup>

We have proposed a depolymerization index (DI) based on the deconvolution of UV fluorescence peaks<sup>46</sup>. It relates the signal of the depolymerization products (monomers and oligomers) to the global signal (products + lignin). This DI is presented in figure 5 for the 3 catalysts and as a function of conversion time for the liquids sampled under isothermal conditions (250°C).

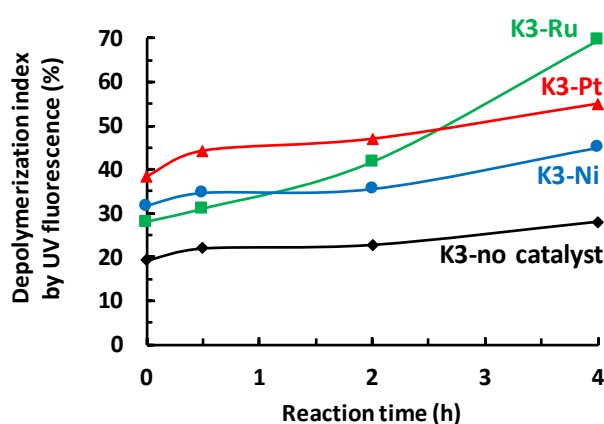


Figure 5. Evolution of the depolymerization index (DI) determined by UV fluorescence for K3 lignin conversion with the 3 catalysts and as a function of reaction time (sampling at 250°C)

The DI (figure 5) is clearly different between catalyzed and uncatalyzed experiments. The DI is much higher in the early stage of the conversion for the 3 catalysts compared to the uncatalyzed experiment. Pt/C presents a higher DI than Ru and Ni/C. Ru/C exhibits a higher increase in DI and overtakes the 2 other catalysts after 4 hours conversion time. This catalyst better promotes the depolymerization of lignin to form oligomers compared to the 2 other catalysts but it does not significantly promote the formation of monomers (based on GC/MS).

In order to gain better insights into the effect of the catalysts, the molecular composition of the monomers was analyzed by GC/MS. The detailed GC/MS results are presented in supplementary material (table S6).

Figure 6 shows that Ru and Pt/C catalysts produce more alkyl phenolic monomers than Ni/C catalyst. It is known that Ni/C presents a lower catalytic activity for hydrogenation reactions.<sup>60</sup> Pt/C exhibits the best selectivity in alkyl phenols.

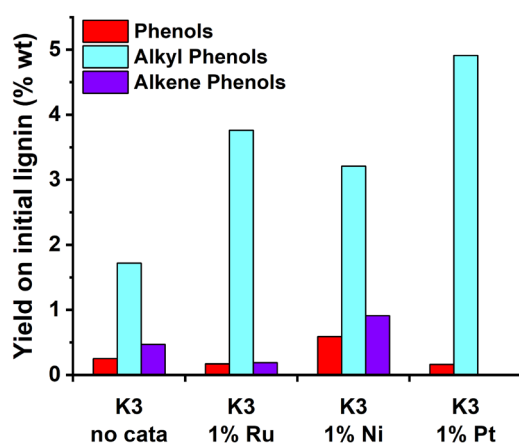


Figure 6. Alkyl, alkene & not substituted phenols yields (wt.%) for after 4h of K3 lignin conversion (250°C, ethanol, H<sub>2</sub>, after 4hours of reaction)

Figure 7 displays the mass yields of the main monomers after 4 hours of K3 lignin conversion.

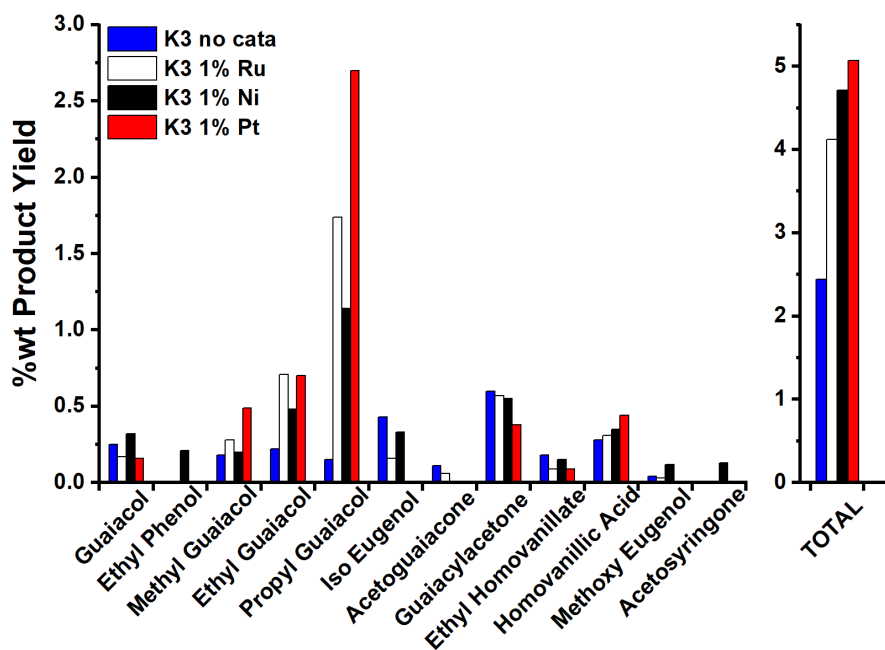


Figure 7. Mass yields (wt.%) of major monomers (by GC/MS) after 4hours of K3 lignin depolymerization (3 catalysts, 250°C, ethanol, H<sub>2</sub>)

It is interesting to notice that the Pt and Ru/C catalysts promote the formation of propyl guaiacol by a factor of more than 10 despite their relatively low mass ratio (1wt.% of metal vs. the mass of lignin). Ethyl guaiacol is also notably promoted by the 3 catalysts. More important differences on monomers yields between the catalyzed and uncatalyzed conditions are obtained in our case compared to Kim et al.<sup>29</sup> probably due to milder conditions (250°C vs. 350°C for Kim et al.) which may enhance the effect of the catalysts.

All the main monomers are composed of guaiacyl groups. It is consistent with the NMR analysis of the K3 lignin (table 2) which is produced by Pine pulping. The alkyl-guaiacols may have some potential

interest as a green solvent in biorefineries<sup>62</sup> or for higher added-value application after purification.<sup>63,64</sup> But they are still produced at low yields due to the recalcitrance of the Kraft lignin.

In order to better understand the formation of these molecules, the evolution of the main monomers sampled upon the time of conversion is presented in figure 8.

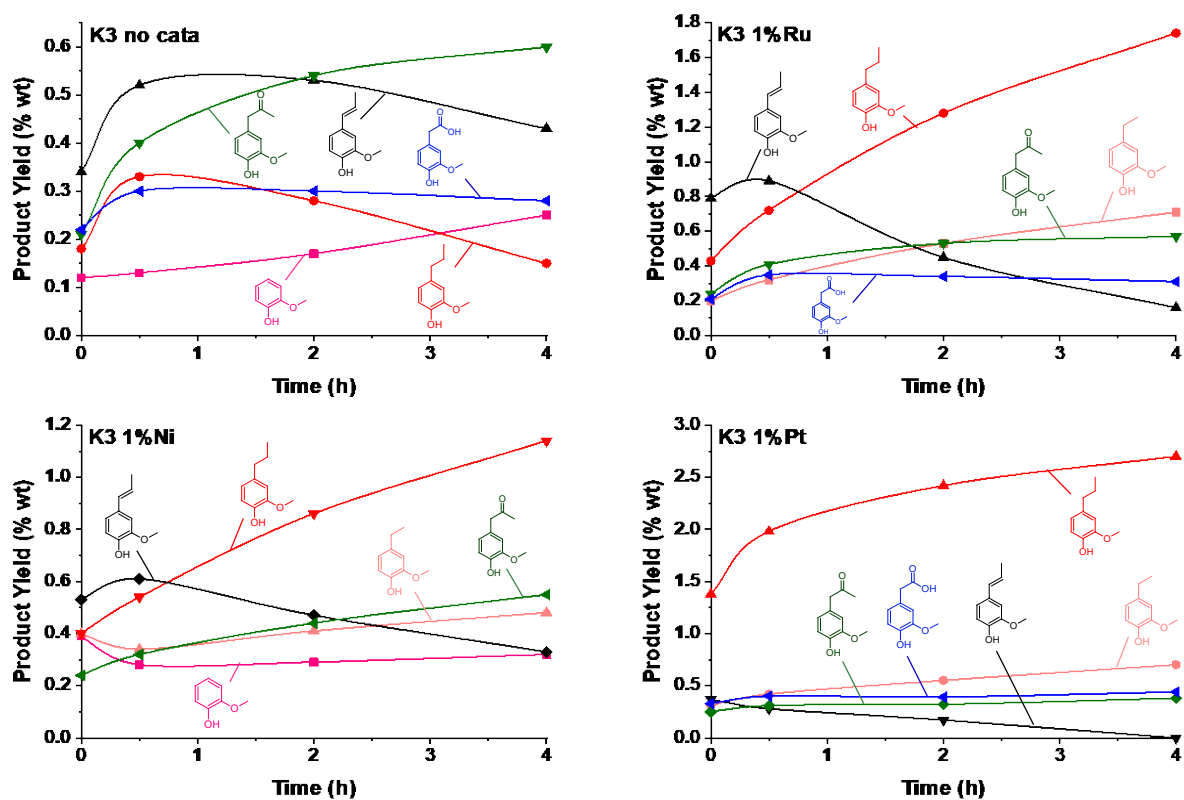


Figure 8. Main monomers as a function of conversion time and catalysts (lignin K3, conversion at 250°C, ethanol, H<sub>2</sub>)

Concerning the uncatalyzed experiment, the methoxyphenols with a ketone or a carboxylic side chain remain stable and the major products. These compounds may be formed by the cleavage of  $\beta$ -O-4 linkages through H-transfer hydrogenolysis of an intermediate pentacyclic ether bond.<sup>56</sup> This reaction occurs at the beginning of the reaction (in the first 30 min) and even without catalyst, under our conditions (figure 8).

The 3 catalysts completely modify the profile of monomers formation. The Ni- and Ru-based catalysts present a similar behaviour with a progressive increase of propyl-guaiacol upon the time of conversion at the expense of isoeugenol. Nevertheless, Ru/C shows a higher ability to hydrogenate the propenyl chain of isoeugenol than the Ni/C catalyst. Pt/C exhibits a different behaviour with propyl-guaiacol being the major component at the early stage of conversion. This results confirms the highest activity of Pt/C to promote H-transfers<sup>29,46</sup> and the subsequent hydrogenation of the alkene side chains. This mechanism has been previously unravelled by Besse et al.<sup>65</sup> The C=C double bond of the propenyl chain in eugenol is fastly hydrogenated by Pt/C. The reaction can be described by a two-step process. The first step is the isomerization of the double bond on the alkyl chain of eugenol. The second step is the hydrogenation of this double bond. Hydrogen can be supplied by ethanol through the Pt active site.<sup>65</sup>

Some ethanol-derived products were detected only at early reaction times and at small yields (1-Butanol; 1,1-diethoxy-Ethane; Butanoic acid, ethyl ester, etc.)<sup>46</sup>. The conversion of ethanol under similar conditions has been studied in more details by other authors<sup>50,66</sup>. It is well known that metallic catalysts enhance the key role of ethanol to stabilize the radical fragments by ethanol alkylation reactions and therefore to promote monomer yields.<sup>31,67</sup>

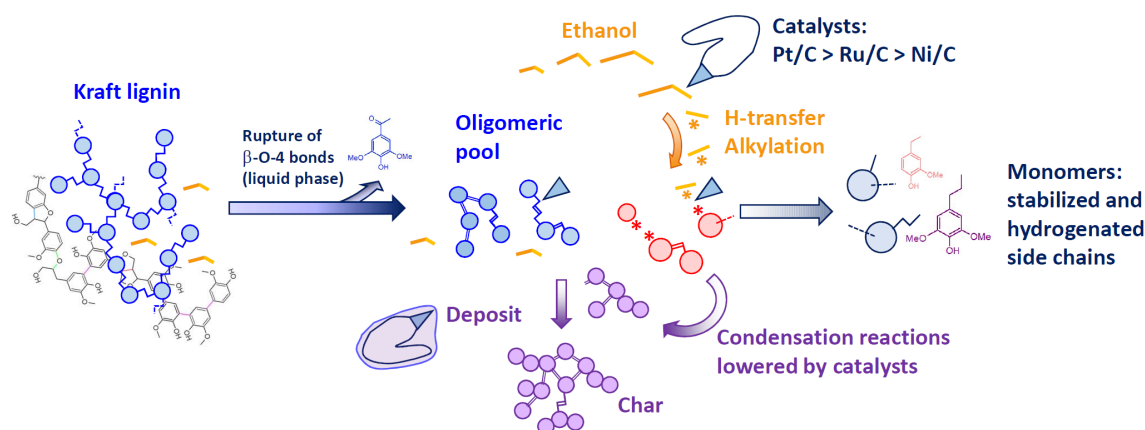


Figure 9. Simplified mechanism of Kraft lignin depolymerization under supercritical ethanol highlighting the different effects of the catalysts (Ni, Ru, Pt/C)

Our main findings concerning this section on the effect of catalysts are summarized in the scheme of figure 9. They are the followings:

- 1) we showed by SEM-EDX and N<sub>2</sub> sorption that all catalysts were recovered by a lignin-based deposit leading to pores plugging.
- 2) For the 3 catalysts, an oligomeric pool prevails as highlighted by GPC and UV fluorescence. The formation of this pool is notably promoted by the catalysts.
- 3) Less deposit is observed over Pt/C which is consistent with a lower char formation. This catalyst promotes the cracking of lignin to oligomers (as evidenced by UV fluorescence) maybe due to a higher activity for C-C bonds cracking than the 2 other catalysts<sup>68</sup>.
- 4) The catalysts (and notably Pt/C) also promote H-transfer reactions to stabilise the broken bonds, reduce condensation reactions and therefore promote monomers formation. They present an important effect on the yield in monomers and notably on propyl-guaiacol by catalysing the hydrogenation of alkene side chains of monomers (like iso-eugenol). But the yield in monomers are still low under our mild conditions whatever the catalysts used due to the recalcitrance of our Kraft lignin.

### 3.4. Effect of technical lignin structure on their depolymerization products with Ni/C

It is important to better understand the effect of the structure of the technical lignins on the depolymerization mechanisms presented in figure 9. Ni/C catalyst has been selected to compare the different lignins because it presents a similar yield in monomers as the other catalysts but with a cheaper and less precious metal (than Pt or Ru). Furthermore, it has been widely used for the depolymerization of various lignins or model compounds <sup>29,42,60,69–71</sup>.

Table 5 presents the char and monomer yields for the 4 different lignins fully characterized in table 2.

Table 5. Yields of char and monomers after 4 hours conversion (250°C, ethanol) for the 4 lignins

Type of lignin	K3	K1	K2	Soda
Catalyst	1% Ni	1% Ni	1% Ni	1% Ni
Char (%wt)	27.7	32.8	10.0	26.1
Monomers (%wt)	4.7	2.2	4.2	4.9

The char yield is 3 times lower (10wt.%) for the K2 lignin. This point may be explained by the combination of a lower molecular weight and higher  $\beta$ -O-4 content of this K2 lignin. These 2 structural behaviours are integrated in the calculation of the theoretical monomer yield (TMY) (see table 2)<sup>26</sup>. K2 presents the highest TMY. Nevertheless, Figure 10 clearly shows that the char yield is not related to the TMY for these 4 lignins (nor to their molecular weight).

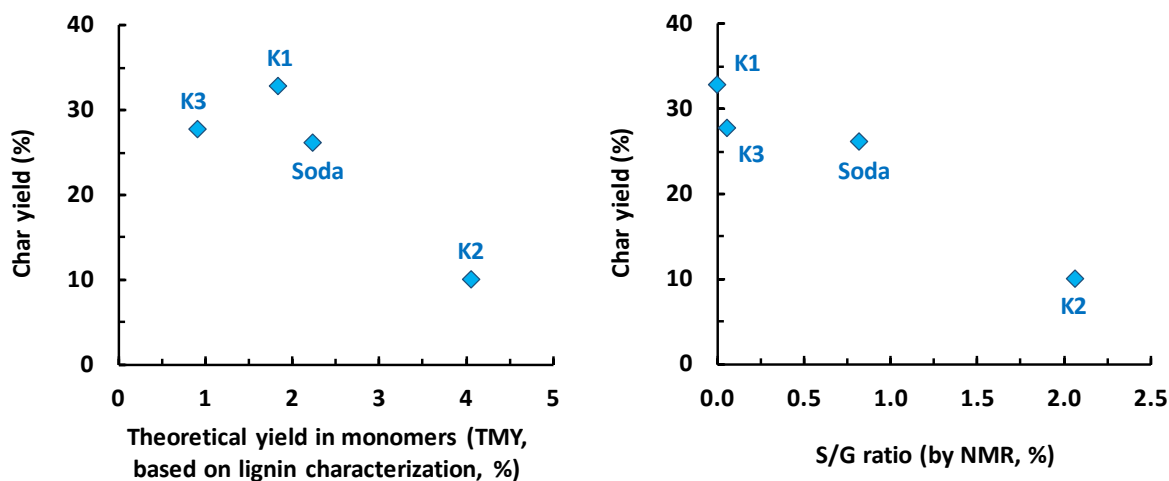


Figure 10. Relations between char yields and the chemical structure of lignins (TMY and S/G ratio)

Char yield can also depend on the S/G ratio of the lignins <sup>61</sup>. Indeed, char formation may rely on the chemistry of the methoxyl groups<sup>61,72</sup>. A possible pathway to char formation from methoxyl aromatic moieties first involves the formation of radical species leading to o-quinone methide and their subsequent polycondensation <sup>61,72</sup>. Syringyl groups are prone to produce more char than guaiacyl ones (roughly twice) because their two methoxyl groups result to a “double opportunity” of o-quinone methide formation. But it remains unclear if this mechanism occurs under catalytic supercritical ethanol conditions. For this reason, we have plotted in figure 10 char yields as a function of the S/G ratio of the 4 lignins (as

quantified by NMR). Char yields decreases with the S/G ratio in lignins. In fact, the methoxyl groups seem mostly stable under our conditions as exemplified in Figure 11 by the excellent correlation between S/G moieties in monomers (by GC/MS) and S/G ratio in lignins (by NMR). Char formation may not be controlled by the conversion of methoxyl groups under our conditions. In the conditions of stable methoxyl groups, it is known that the 5-position on the aromatic ring in guaiacyl group is more susceptible to condensation reactions.<sup>73</sup> Therefore, the char yield may rather depend on guaiacyl group contents in our conditions (figure 10).

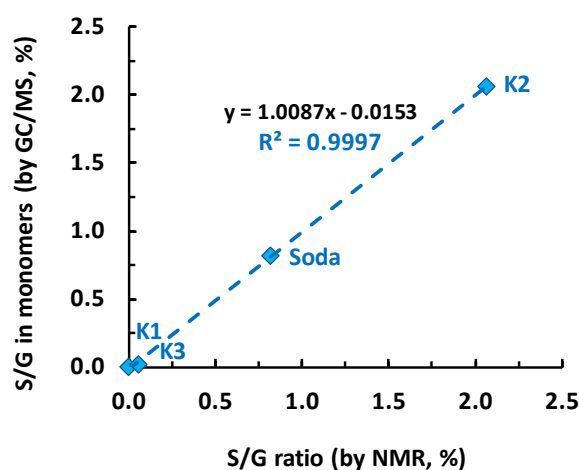


Figure 11. Relations between the S/G moieties present in all quantified monomers (by GC/MS, %mol.) and the S/G ratio quantified by NMR in the lignins (% mol.)

Figure 12 shows that the monomer final yield is not related to the TMY of the lignins, under our conditions, contrary to previous studies<sup>42–45</sup> using less condensed lignins and/or lignins presenting a larger range of  $\beta$ -O-4 content. In our case, the monomer yield is not related either to other ether bonds cleavage nor to the S/G ratio.

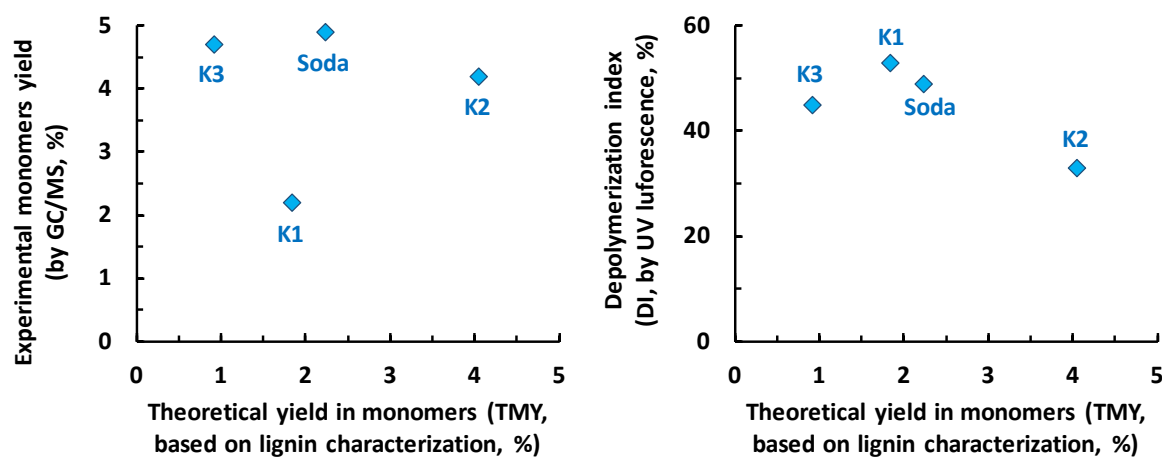


Figure 12. Lack of relation between experimental monomers yield, depolymerization index and theoretical yield in monomers

The UV fluorescence spectra and index are presented in supporting material (figure S14 and S15). It shows a higher depolymerization for K1 and Soda lignins after 4 hours' conversion. K2 seems the most recalcitrant lignin based on UV fluorescence. This point may be tentatively explained by a lower content in

aliphatic carbons (by  $^{13}\text{C}$  NMR, table 2) in K2 lignin leading to lower available bonds for C-C catalytic cracking. The catalyst may cleave C-C bonds<sup>29,50</sup> (probably rather saturated, less stable). The lower yield in C-C bond conversion for K2 may also reduce the subsequent re-condensation reactions leading to char. As for monomer yields, the depolymerization index (DI) is not related to the conversion of  $\beta\text{-O-4}$  bonds (to TMY, figure 12). The lignin structure highly impacts the relative distribution in oligomers (notably for K2) but not their average molecular size. Indeed, GPC analysis (table S5) shows similar molecular size of the liquids (about 800-900 Da) in agreement with the constant emission wavelength (around 350nm) of the oligomers peak obtained by UV fluorescence (figure S14).

Monomer and oligomers yields are not controlled by the cleavage of  $\beta\text{-O-4}$  bonds in our conditions. It may rather depend on the behaviour of the catalyst to cleave other bonds (notably C-C bonds<sup>29,50</sup>) and to stabilise the formed fragments by H-transfers. Other yet unexplored phenomena may also occur<sup>13,61</sup> such as: the branching of lignin macromolecules, the conformation of lignin and oligomeric pool in the solvent, mass transfer effects, the accessibility of lignin bonds to the active sites of the catalyst, etc.

The global monomer yields are not well related to lignin structure. Nevertheless, the chemical composition of the monomers is highly impacted by the lignin structure, as displayed in figure 11 for the S/G ratio of monomers.

Figure 13 presents the main chemical families of phenolic monomers for the 4 lignins.

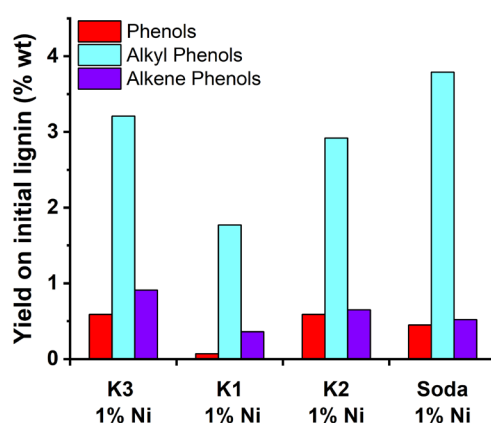


Figure 13. Alkyl, alkene & not substituted phenols yields (wt.%) for the 4 different lignins after 4h conversion time (Ni/C, 250°C, ethanol)

The 4 lignins produce mainly alkyl phenols. Ni/C catalyst can promote the hydrogenation of the side chains<sup>60</sup> and the ethanol-based alkylation of monomeric fragments<sup>31,50</sup>. K1 produces a very low yield in unsubstituted phenols. We did not succeed to explain this result based on the structural analysis of this lignin.

Figure 14 presents the breakdown of major monomers. K2 and Soda lignins form an important yield in propyl-syringol, which is in-line with their higher syringyl content as analyzed by NMR. Syringol and propyl syringol are not detected for K1 and K3 lignins. The K3 lignin produces the highest yield in propyl guaiacol.

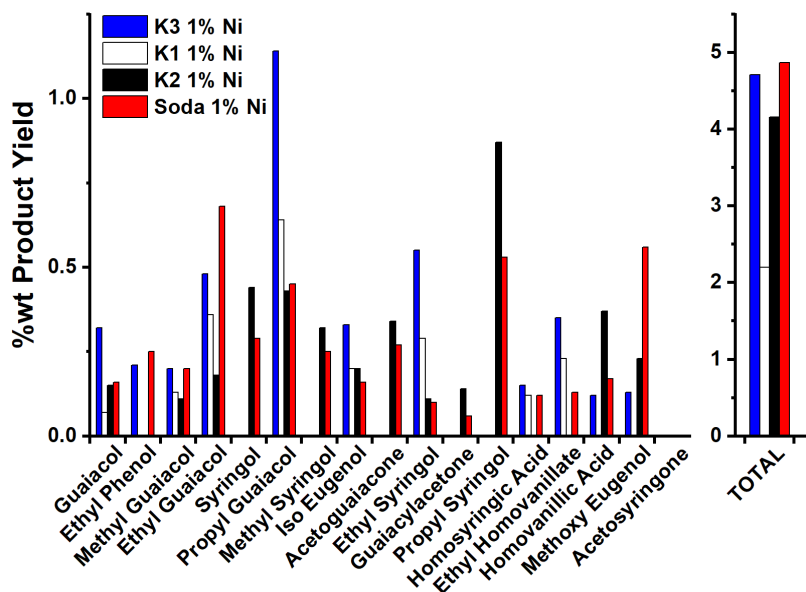


Figure 14. Mass yields of major monomers for the 4 lignins with Ni/C catalyst after 4 hours of conversion

In order to better understand the fate of these major monomers, their profile is displayed as a function of time in figure 15.

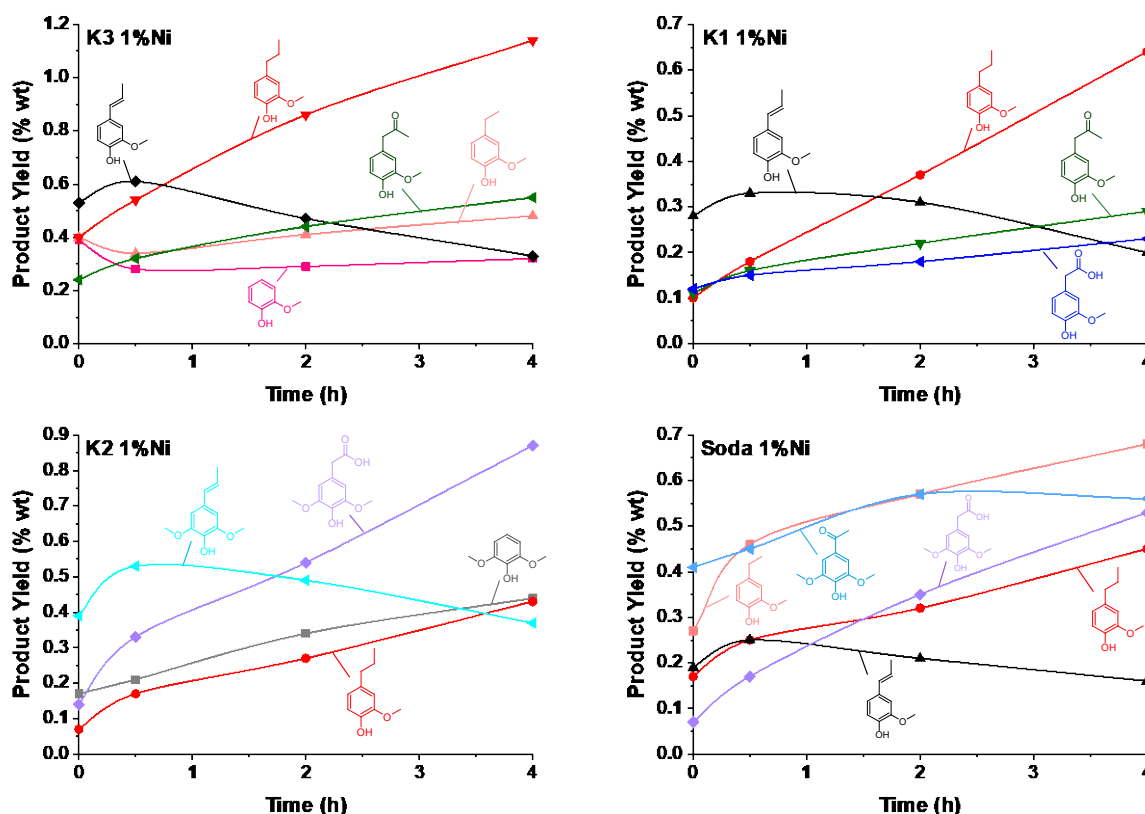


Figure 15. Main monomers as a function of conversion time (different lignins, Ni/C, conversion at 250°C, ethanol, H<sub>2</sub>)

For all lignins, alkene phenols are first formed probably by C-C bonds cracking and then hydrogenated. Alkyl guaiacols are progressively formed for all lignins. K3 and K1 lignins present similar patterns for the

monomer formation profiles with a progressive increase in propylguaiacol. This major compound is related to their higher guaiacyl content. Soda and K2 lignins exhibit a different behaviour than K3 and K1 producing more syringyl monomers. The carboxylic acid side chain in the homosyringic acid is progressively formed for K2 and Soda lignins. Its mechanism of formation is still unclear.

Our main findings concerning the effect of lignin structure on the depolymerization mechanisms and products are summarized in figure 16.

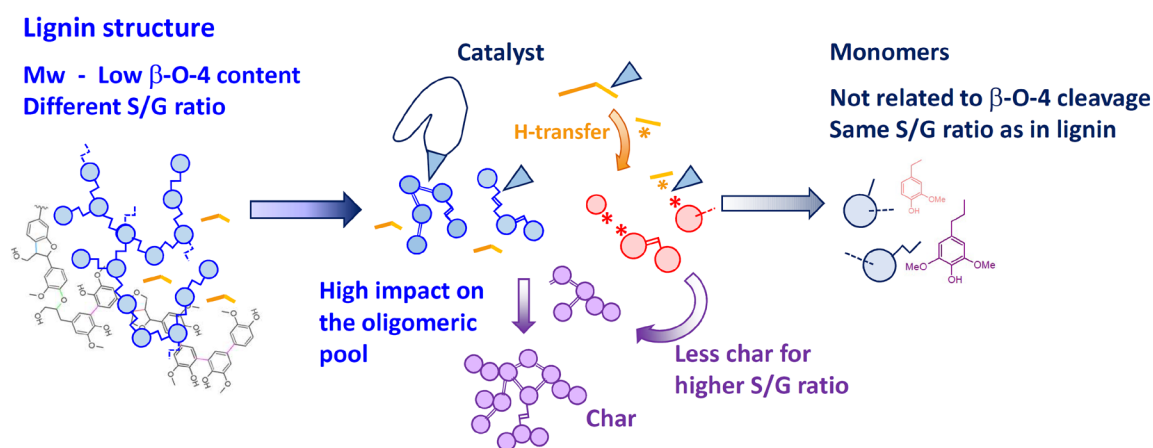


Figure 16. Simplified mechanism of technical lignins depolymerization under supercritical ethanol highlighting the effects of lignin structures (with Ni/C catalyst)

We have shown that:

- 1) The monomers yield is not related to the cleavage of  $\beta$ -O-4 bonds for such condensed lignins;
- 2) The S/G ratio in monomers is very well related to the S/G ratio of the lignins implying that methoxyl groups are mostly stable under our conditions;
- 3) Char yield seems to be reduced for higher S/G ratio lignins;
- 4) The oligomeric pool is still predominant for all lignins with a global similar molecular weight (Mw  $\sim$ 800 Da) but with different behaviours between lignins (maybe related to different aliphatic contents).

#### 4. Conclusion

The main results of this work are the followings:

- 1) 3 commercial catalysts (Ni, Ru, Pt/C) were characterized before and after lignin depolymerization by  $N_2$  sorption, XRD, TEM and SEM. They all present an important plugging of pores with a deposit of a lignin-based carbonaceous over the catalyst particles. Therefore, cheap catalysts and with large pores must be looked for to depolymerize lignin. For instance, the as-produced lignin char may be an interesting support for low cost metals (like iron)<sup>18</sup>.
- 2) The 3 catalysts promote significantly the production of monomers and notably of propyl-guaiacol. They promote the hydrogenation of the side chains of the monomers. But the monomer yields are still low (<5wt.%) for all catalysts.

- 3) An important oligomeric pool dominates the composition of the liquids (as analyzed by UV fluorescence and GPC analysis) for all conditions.
- 4) All our technical lignins present a highly condensed structure with a low content in ether bonds. The relation between  $\beta$ -O-4 bonds cleavage and monomer yields established by previous studies (on a larger range of ether bond contents) does not perform for these technical lignins (under our conditions).
- 5) Important differences between lignins are evidenced on the formation profile of some monomers and notably on syringyl/guaiacyl species which are well related to the S/G ratio of lignins (as analyzed by NMR).

Concerning the perspectives of this work, the monomers yields should be increased by keeping a manageable pressure for industrial reactors ( $\sim 100$  Bars limiting the temperature to about  $250^{\circ}\text{C}$  for supercritical ethanol). More efficient and low cost catalysts must be looked for to promote monomers. Alternatively, other solvents than ethanol could be used. For instance, the as-produced lignin oil (as in the Noguchi process) could act as an internal solvent and capping agent. It enables higher temperature to better activate C-C bond cleavage but by keeping a global liquid state in the reactor, which is favourable to promote H-transfers.

Considering the high recalcitrance of the technical lignins, the target for pulp mills could be to quest profitable and complementary markets for the 3 main products of lignin depolymerization: monomers, oligomers and char.

## 5. Supporting information

The supporting information file presents: 1) literature review; 2) lignin precipitation from black liquor; 3) characterization of lignins (GPC, NMR); 4) characterization of catalysts (SEM/EDx, XRD, pores distribution); 5) analysis of liquids (methods and more detailed results for GC/MS and UV fluorescence spectra).

## 6. Fundings

This work was supported by ANR through the project “PhenoLiq”.

## 7. References

- (1) Ragauskas, A. J.; Beckham, G. T.; Bidy, M. J.; Chandra, R.; Chen, F.; Davis, M. F.; Davison, B. H.; Dixon, R. A.; Gilna, P.; Keller, M.; Langan, P.; Naskar, A. K.; Saddler, J. N.; Tschaplinski, T. J.; Tuskan, G. A.; Wyman, C. E. Lignin Valorization: Improving Lignin Processing in the Biorefinery. *Science* **2014**, *344* (6185), 1246843–1246843. <https://doi.org/10.1126/science.1246843>.
- (2) Lignin Market Size & Share | Industry Report, 2020-2027 <https://www.grandviewresearch.com/industry-analysis/lignin-market> (accessed 2021 -08 -03).
- (3) Xu, C. C.; Dessbesell, L.; Zhang, Y.; Yuan, Z. Lignin Valorization beyond Energy Use: Has Lignin’s Time Finally Come? *Biofuels, Bioproducts and Biorefining* **2021**, *15* (1), 32–36. <https://doi.org/10.1002/bbb.2172>.
- (4) Axelsson, E.; Olsson, M. R.; Berntsson, T. Increased Capacity in Kraft Pulp Mills: Lignin Separation and Reduced Steam Demand Compared with Recovery Boiler Upgrade. **2006**. <https://doi.org/10.3183/nppri-2006-21-04-p485-492>.

- (5) Lundberg, V.; Svensson, E.; Mahmoudkhani, M.; Axelsson, E. Converting a Kraft Pulp Mill into a Multi-Product Biorefinery – Part 2: Economic Aspects. *Nordic Pulp & Paper Research Journal* **2013**, *28* (4), 489–497. <https://doi.org/10.3183/npprj-2013-28-04-p489-497>.
- (6) Tomani, P. The LignoBoost Process. *Cellulose Chemistry and Technology* **2010**, *44* (1–3), 53–58.
- (7) Crestini, C.; Lange, H.; Sette, M.; Argyropoulos, D. S. On the Structure of Softwood Kraft Lignin. *Green Chem.* **2017**, *19* (17), 4104–4121. <https://doi.org/10.1039/C7GC01812F>.
- (8) Giummarella, N.; Lindén, P. A.; Areskog, D.; Lawoko, M. Fractional Profiling of Kraft Lignin Structure: Unravelling Insights on Lignin Reaction Mechanisms. *ACS Sustainable Chem. Eng.* **2020**, *8* (2), 1112–1120. <https://doi.org/10.1021/acssuschemeng.9b06027>.
- (9) Zakzeski, J.; Bruijninx, P. C. A.; Jongerius, A. L.; Weckhuysen, B. M. The Catalytic Valorization of Lignin for the Production of Renewable Chemicals. *Chemical Reviews* **2010**, *110* (6), 3552–3599. <https://doi.org/10.1021/cr900354u>.
- (10) Rinaldi, R.; Jastrzebski, R.; Clough, M. T.; Ralph, J.; Kennema, M.; Bruijninx, P. C. A.; Weckhuysen, B. M. Paving the Way for Lignin Valorisation: Recent Advances in Bioengineering, Biorefining and Catalysis. *Angewandte Chemie International Edition* **2016**, *55* (29), 8164–8215. <https://doi.org/10.1002/anie.201510351>.
- (11) Schutyser, W.; Renders, T.; Van den Bosch, S.; Koelewijn, S.-F.; Beckham, G. T.; Sels, B. F. Chemicals from Lignin: An Interplay of Lignocellulose Fractionation, Depolymerisation, and Upgrading. *Chemical Society Reviews* **2018**, *47* (3), 852–908. <https://doi.org/10.1039/C7CS00566K>.
- (12) Holladay, J. E.; Bozell, J. J.; White, J. F.; Johnson, D. Top Value-Added Chemicals from Biomass. *DOE Report PNNL* **2007**, 16983.
- (13) Terrell, E.; Dellon, L. D.; Dufour, A.; Bartolomei, E.; Broadbelt, L. J.; Garcia-Perez, M. A Review on Lignin Liquefaction: Advanced Characterization of Structure and Microkinetic Modeling. *Ind. Eng. Chem. Res.* **2020**, *59* (2), 526–555. <https://doi.org/10.1021/acs.iecr.9b05744>.
- (14) Olcese, R. N.; Francois, J.; Bettahar, M. M.; Petitjean, D.; Dufour, A. Hydrodeoxygenation of Guaiacol, A Surrogate of Lignin Pyrolysis Vapors, Over Iron Based Catalysts: Kinetics and Modeling of the Lignin to Aromatics Integrated Process. *Energy Fuels* **2013**, *27* (2), 975–984. <https://doi.org/10.1021/ef301971a>.
- (15) de Wild, P.; Van der Laan, R.; Kloekhorst, A.; Heeres, E. Lignin Valorisation for Chemicals and (Transportation) Fuels via (Catalytic) Pyrolysis and Hydrodeoxygenation. *Environ. Prog. Sustainable Energy* **2009**, *28* (3), 461–469. <https://doi.org/10.1002/ep.10391>.
- (16) Gonzalez-Borja, M. A.; Resasco, D. E. Anisole and Guaiacol Hydrodeoxygenation over Monolithic Pt-Sn Catalysts. *Energy Fuels* **2011**, *25* (9), 4155–4162.
- (17) Zhao, H. Y.; Li, D.; Bui, P.; Oyama, S. T. Hydrodeoxygenation of Guaiacol as Model Compound for Pyrolysis Oil on Transition Metal Phosphide Hydroprocessing Catalysts. *Appl. Catal. A* **2011**, *391* (1–2), 305–310. <https://doi.org/10.1016/j.apcata.2010.07.039>.
- (18) Olcese, R. N.; Lardier, G.; Bettahar, M.; Ghanbaja, J.; Fontana, S.; Carré, V.; Aubriet, F.; Petitjean, D.; Dufour, A. Aromatic Chemicals by Iron-Catalyzed Hydrotreatment of Lignin Pyrolysis Vapor. *ChemSusChem* **2013**, *6* (8), 1490–1499. <https://doi.org/10.1002/cssc.201300191>.
- (19) Lago, V.; Briens, C.; Berruti, F. Effect of Bed Material, Lignin Content, and Origin on the Processability of Biomass in Fast Pyrolysis Reactors. *The Canadian Journal of Chemical Engineering* **2018**, *96* (1), 132–144. <https://doi.org/10.1002/cjce.22932>.
- (20) Meier, D.; Berns, J.; Faix, O.; Balfanz, U.; Baldauf, W. Hydrocracking of Organocell Lignin for Phenol Production. *Biomass and Bioenergy* **1994**, *7* (1), 99–105. [https://doi.org/10.1016/0961-9534\(95\)92632-I](https://doi.org/10.1016/0961-9534(95)92632-I).
- (21) Agarwal, S.; Chowdari, R. K.; Hita, I.; Heeres, H. J. Experimental Studies on the Hydrotreatment of Kraft Lignin to Aromatics and Alkylphenolics Using Economically Viable Fe-Based Catalysts. *ACS Sustainable Chem. Eng.* **2017**, *5* (3), 2668–2678. <https://doi.org/10.1021/acssuschemeng.6b03012>.
- (22) Goheen, D. Hydrogenation of Lignin by the Noguchi Process. In *Lignin Structure and Reactions*; Advances in Chemistry; 1966; Vol. 59, pp 205–225.
- (23) Elliott, D. C.; Beckman, D.; Bridgewater, A. V.; Diebold, J. P.; Gevert, S. B.; Solantausta, Y. Developments in Direct Thermochemical Liquefaction of Biomass: 1983–1990. *Energy Fuels* **1991**, *5* (3), 399–410. <https://doi.org/10.1021/ef00027a008>.
- (24) Shabtai, J. S.; Zmierczak, W. W.; Chornet, E.; Johnson, D. Process for Converting Lignins into a High Octane Blending Component. Patent US20030115792, 2003.

- (25) Liu, X.; Bouxin, F. P.; Fan, J.; Budarin, V. L.; Hu, C.; Clark, J. H. Recent Advances in the Catalytic Depolymerization of Lignin towards Phenolic Chemicals: A Review. *ChemSusChem* **2020**, *13* (17), 4296–4317. <https://doi.org/10.1002/cssc.202001213>.
- (26) Tricker, A. W.; Stellato, M. J.; Kwok, T. T.; Kruyer, N. S.; Wang, Z.; Nair, S.; Thomas, V. M.; Realff, M. J.; Bommarius, A. S.; Sievers, C. Similarities in Recalcitrant Structures of Industrial Non-Kraft and Kraft Lignin. *ChemSusChem* **2020**, *13* (17), 4624–4632. <https://doi.org/10.1002/cssc.202001219>.
- (27) Dessbesell, L.; Yuan, Z.; Leitch, M.; Paleologou, M.; Pulkki, R.; Xu, C. C. Capacity Design of a Kraft Lignin Biorefinery for Production of Biophenol via a Proprietary Low-Temperature/Low-Pressure Lignin Depolymerization Process. *ACS Sustainable Chem. Eng.* **2018**, *6* (7), 9293–9303. <https://doi.org/10.1021/acssuschemeng.8b01582>.
- (28) Feghali, E.; van de Pas, D. J.; Torr, K. M. Toward Bio-Based Epoxy Thermoset Polymers from Depolymerized Native Lignins Produced at the Pilot Scale. *Biomacromolecules* **2020**, *21* (4), 1548–1559. <https://doi.org/10.1021/acs.biomac.0c00108>.
- (29) Kim, J.-Y.; Park, J.; Kim, U.-J.; Choi, J. W. Conversion of Lignin to Phenol-Rich Oil Fraction under Supercritical Alcohols in the Presence of Metal Catalysts. *Energy & Fuels* **2015**, *29* (8), 5154–5163. <https://doi.org/10.1021/acs.energyfuels.5b01055>.
- (30) Huang, X.; Atay, C.; Korányi, T. I.; Boot, M. D.; Hensen, E. J. M. Role of Cu–Mg–Al Mixed Oxide Catalysts in Lignin Depolymerization in Supercritical Ethanol. *ACS Catalysis* **2015**, *5* (12), 7359–7370. <https://doi.org/10.1021/acscatal.5b02230>.
- (31) Huang, X.; Korányi, T. I.; Boot, M. D.; Hensen, E. J. M. Ethanol as Capping Agent and Formaldehyde Scavenger for Efficient Depolymerization of Lignin to Aromatics. *Green Chemistry* **2015**, *17* (11), 4941–4950. <https://doi.org/10.1039/C5GC01120E>.
- (32) Huang, X.; Korányi, T. I.; Boot, M. D.; Hensen, E. J. M. Catalytic Depolymerization of Lignin in Supercritical Ethanol. *ChemSusChem* **2014**, *7* (8), 2276–2288. <https://doi.org/10.1002/cssc.201402094>.
- (33) Huang, X.; Atay, C.; Zhu, J.; Palstra, S. W. L.; Korányi, T. I.; Boot, M. D.; Hensen, E. J. M. Catalytic Depolymerization of Lignin and Woody Biomass in Supercritical Ethanol: Influence of Reaction Temperature and Feedstock. *ACS Sustainable Chemistry & Engineering* **2017**, *5* (11), 10864–10874. <https://doi.org/10.1021/acssuschemeng.7b02790>.
- (34) Wildschut, J.; Mahfud, F. H.; Venderbosch, R. H.; Heeres, H. J. Hydrotreatment of Fast Pyrolysis Oil Using Heterogeneous Noble-Metal Catalysts. *Ind. Eng. Chem. Res.* **2009**, *48* (23), 10324–10334. <https://doi.org/10.1021/ie9006003>.
- (35) Kozliak, E. I.; Kubátová, A.; Artemyeva, A. A.; Nagel, E.; Zhang, C.; Rajappagowda, R. B.; Smirnova, A. L. Thermal Liquefaction of Lignin to Aromatics: Efficiency, Selectivity, and Product Analysis. *ACS Sustainable Chemistry & Engineering* **2016**, *4* (10), 5106–5122. <https://doi.org/10.1021/acssuschemeng.6b01046>.
- (36) Gilkey, M. J.; Xu, B. Heterogeneous Catalytic Transfer Hydrogenation as an Effective Pathway in Biomass Upgrading. *ACS Catal.* **2016**, *6* (3), 1420–1436. <https://doi.org/10.1021/acscatal.5b02171>.
- (37) Nielsen, J. B.; Jensen, A.; Madsen, L. R.; Larsen, F. H.; Felby, C.; Jensen, A. D. Noncatalytic Direct Liquefaction of Biorefinery Lignin by Ethanol. *Energy Fuels* **2017**, *31* (7), 7223–7233. <https://doi.org/10.1021/acs.energyfuels.7b00968>.
- (38) Jones, S. B. Production of Gasoline and Diesel from Biomass via Fast Pyrolysis, Hydrotreating and Hydrocracking: A Design Case. *PNNL report N°8284* **2009**, 76.
- (39) A. Nicolae, S.; Au, H.; Modugno, P.; Luo, H.; E. Szego, A.; Qiao, M.; Li, L.; Yin, W.; J. Heeres, H.; Berge, N.; Titirici, M.-M. Recent Advances in Hydrothermal Carbonisation: From Tailored Carbon Materials and Biochemicals to Applications and Bioenergy. *Green Chemistry* **2020**, *22* (15), 4747–4800. <https://doi.org/10.1039/D0GC00998A>.
- (40) de Wild, P. J.; Huijgen, W. J. J.; Kloekhorst, A.; Chowdari, R. K.; Heeres, H. J. Biobased Alkylphenols from Lignins via a Two-Step Pyrolysis – Hydrodeoxygenation Approach. *Bioresource Technology* **2017**, *229*, 160–168. <https://doi.org/10.1016/j.biortech.2017.01.014>.
- (41) Cabral Almada, C.; Kazachenko, A.; Fongarland, P.; Da Silva Perez, D.; Kuznetsov, B. N.; Djakovitch, L. Oxidative Depolymerization of Lignins for Producing Aromatics: Variation of Botanical Origin and Extraction Methods. *Biomass Conv. Bioref.* **2020**. <https://doi.org/10.1007/s13399-020-00897-6>.
- (42) Phongpreecha, T.; Hool, N. C.; Stoklosa, R. J.; Klett, A. S.; Foster, C. E.; Bhalla, A.; Holmes, D.; Thies, M. C.; Hodge, D. B. Predicting Lignin Depolymerization Yields from Quantifiable Properties

- Using Fractionated Biorefinery Lignins. *Green Chem.* **2017**, *19* (21), 5131–5143. <https://doi.org/10.1039/C7GC02023F>.
- (43) Amiri, M. T.; Bertella, S.; Questell-Santiago, Y. M.; Luterbacher, J. S. Establishing Lignin Structure–Upgradeability Relationships Using Quantitative  $1\text{H}$ – $13\text{C}$  Heteronuclear Single Quantum Coherence Nuclear Magnetic Resonance (HSQC-NMR) Spectroscopy. *Chem. Sci.* **2019**, *10* (35), 8135–8142. <https://doi.org/10.1039/C9SC02088H>.
- (44) Wang, S.; Li, W.-X.; Yang, Y.-Q.; Chen, X.; Ma, J.; Chen, C.; Xiao, L.-P.; Sun, R.-C. Unlocking Structure–Reactivity Relationships for Catalytic Hydrogenolysis of Lignin into Phenolic Monomers. *ChemSusChem* **2020**, *13* (17), 4548–4556. <https://doi.org/10.1002/cssc.202000785>.
- (45) Bouxin, F. P.; McVeigh, A.; Tran, F.; Westwood, N. J.; Jarvis, M. C.; Jackson, S. D. Catalytic Depolymerisation of Isolated Lignins to Fine Chemicals Using a Pt/Alumina Catalyst: Part 1—Impact of the Lignin Structure. *Green Chem.* **2015**, *17* (2), 1235–1242. <https://doi.org/10.1039/C4GC01678E>.
- (46) Bartolomei, E.; Le Brech, Y.; Dufour, A.; Carre, V.; Aubriet, F.; Terrell, E.; Garcia-Perez, M.; Arnoux, P. Lignin Depolymerization: A Comparison of Methods to Analyze Monomers and Oligomers. *ChemSusChem* **2020**, *13* (17), 4633–4648. <https://doi.org/10.1002/cssc.202001126>.
- (47) Water Quality -- Determination of Selected Elements by Inductively Coupled Plasma Optical Emission Spectrometry (ICP-OES). *ISO 11885* (2007).
- (48) Constant, S.; Wienk, H. L. J.; Frissen, A. E.; Peinder, P. de; Boelens, R.; van Es, D. S.; Grisel, R. J. H.; Weckhuysen, B. M.; Huijgen, W. J. J.; Gosselink, R. J. A.; Bruijninx, P. C. A. New Insights into the Structure and Composition of Technical Lignins: A Comparative Characterisation Study. *Green Chemistry* **2016**, *18* (9), 2651–2665. <https://doi.org/10.1039/C5GC03043A>.
- (49) Shrestha, B.; le Brech, Y.; Ghislain, T.; Leclerc, S.; Carré, V.; Aubriet, F.; Hoppe, S.; Marchal, P.; Pontvianne, S.; Brosse, N.; Dufour, A. A Multitechnique Characterization of Lignin Softening and Pyrolysis. *ACS Sustainable Chem. Eng.* **2017**, *5* (8), 6940–6949. <https://doi.org/10.1021/acssuschemeng.7b01130>.
- (50) Cheng, C.; Li, P.; Yu, W.; Shen, D.; Jiang, X.; Gu, S. Nonprecious Metal/Bimetallic Catalytic Hydrogenolysis of Lignin in a Mixed-Solvent System. *ACS Sustainable Chem. Eng.* **2020**, *8* (43), 16217–16228. <https://doi.org/10.1021/acssuschemeng.0c05362>.
- (51) Dufour, A.; Celzard, A.; Fierro, V.; Broust, F.; Courson, C.; Zoulalian, A.; Rouzaud, J. N. Catalytic Conversion of Methane over a Biomass Char for Hydrogen Production: Deactivation and Regeneration by Steam Gasification. *Applied Catalysis A: General* **2015**, *490*, 170–180. <https://doi.org/10.1016/j.apcata.2014.10.038>.
- (52) Devi, T. G.; Kannan, M. P. Nickel Catalyzed Air Gasification of Cellulosic Chars Jump in Reactivity. *Energy & Fuels* **2001**, *15*, 583–590. <https://doi.org/10.1021/ef0001540>.
- (53) Baker, R. T. K. The Relationship between Particle Motion on a Graphite Surface and Tamman Temperature. *Journal of Catalysis* **1982**, *78* (2), 473–476. [https://doi.org/10.1016/0021-9517\(82\)90332-3](https://doi.org/10.1016/0021-9517(82)90332-3).
- (54) Hansen, T. W.; DeLaRiva, A. T.; Challa, S. R.; Datye, A. K. Sintering of Catalytic Nanoparticles: Particle Migration or Ostwald Ripening? *Acc. Chem. Res.* **2013**, *46* (8), 1720–1730. <https://doi.org/10.1021/ar3002427>.
- (55) Wynblatt, P.; Gjostein, N. A. Supported Metal Crystallites. *Progress in Solid State Chemistry* **1975**, *9*, 21–58. [https://doi.org/10.1016/0079-6786\(75\)90013-8](https://doi.org/10.1016/0079-6786(75)90013-8).
- (56) Besse, X.; Schuurman, Y.; Guilhaume, N. Reactivity of Lignin Model Compounds through Hydrogen Transfer Catalysis in Ethanol/Water Mixtures. *Applied Catalysis B: Environmental* **2017**, *209*, 265–272. <https://doi.org/10.1016/j.apcatb.2017.03.013>.
- (57) Katoh, T.; Yokoyama, S.; Sanada, Y. Analysis of a Coal-Derived Liquid Using Highpressure Liquid Chromatography and Synchronous Fluorescence Spectrometry. *Fuel* **1980**, *59* (12), 845–850.
- (58) Delpuech, J. J.; Nicole, D.; Cagniant, D.; Cleon, P.; Foucheres, M. C.; Dumay, D.; Aune, J. P.; Genard, A. Characterization of Catalytically Hydrogenated and Pyrolysis Coal Products. A Comparative Study of Several Analytical Procedures. *Fuel processing technology* **1986**, *12*, 205–241.
- (59) Zander, M.; Haenel, M. W. Regularities in the Fluorescence Spectra of Coal-Tar Pitch Fractions. *Fuel* **1990**, *69* (9), 1206–1207. [https://doi.org/10.1016/0016-2361\(90\)90083-3](https://doi.org/10.1016/0016-2361(90)90083-3).
- (60) Bječić, A.; Grilc, M.; Huš, M.; Likozar, B. Hydrogenation and Hydrodeoxygenation of Aromatic Lignin Monomers over Cu/C, Ni/C, Pd/C, Pt/C, Rh/C and Ru/C Catalysts: Mechanisms, Reaction

- Micro-Kinetic Modelling and Quantitative Structure-Activity Relationships. *Chemical Engineering Journal* **2019**, *359*, 305–320. <https://doi.org/10.1016/j.cej.2018.11.107>.
- (61) Terrell, E.; Dellon, L. D.; Dufour, A.; Bartolomei, E.; Broadbelt, L. J.; Garcia-Perez, M. A Review on Lignin Liquefaction: Advanced Characterization of Structure and Microkinetic Modeling. *Industrial & Engineering Chemistry Research* **2020**, *59* (2), 526–555. <https://doi.org/10.1021/acs.iecr.9b05744>.
- (62) Azadi, P.; Carrasquillo-Flores, R.; Pagán-Torres, Y. J.; Gürbüz, E. I.; Farnood, R.; Dumesic, J. A. Catalytic Conversion of Biomass Using Solvents Derived from Lignin. *Green Chem.* **2012**, *14* (6), 1573–1576. <https://doi.org/10.1039/C2GC35203F>.
- (63) Pakdel, H.; De Caumia, B.; Roy, C. Vacuum Pyrolysis of Lignin Derived from Steam-Exploded Wood. *Biomass and Bioenergy* **1992**, *3* (1), 31–40. [https://doi.org/10.1016/0961-9534\(92\)90017-K](https://doi.org/10.1016/0961-9534(92)90017-K).
- (64) Amen-Chen, C.; Pakdel, H.; Roy, C. Production of Monomeric Phenols by Thermochemical Conversion of Biomass: A Review. *Bioresource Technology* **2001**, *79* (3), 277–299. [https://doi.org/10.1016/S0960-8524\(00\)00180-2](https://doi.org/10.1016/S0960-8524(00)00180-2).
- (65) Besse, X.; Schuurman, Y.; Guilhaume, N. Hydrothermal Conversion of Lignin Model Compound Eugenol. *Catalysis Today* **2015**, *258*, 270–275. <https://doi.org/10.1016/j.cattod.2014.12.010>.
- (66) Nielsen, J. B.; Jensen, A.; Schandel, C. B.; Felby, C.; Jensen, A. D. Solvent Consumption in Non-Catalytic Alcohol Solvolysis of Biorefinery Lignin. *Sustainable Energy Fuels* **2017**, *1* (9), 2006–2015. <https://doi.org/10.1039/C7SE00381A>.
- (67) Parto, S. G.; Christensen, J. M.; Pedersen, L. S.; Hansen, A. B.; Tjosås, F.; Spiga, C.; Damsgaard, C. D.; Larsen, D. B.; Duus, J. Ø.; Jensen, A. D. Liquefaction of Lignosulfonate in Supercritical Ethanol Using Alumina-Supported NiMo Catalyst. *Energy Fuels* **2019**, *33* (2), 1196–1209. <https://doi.org/10.1021/acs.energyfuels.8b03519>.
- (68) Bjelić, A.; Likozar, B.; Grilc, M. Scaling of Lignin Monomer Hydrogenation, Hydrodeoxygenation and Hydrocracking Reaction Micro-Kinetics over Solid Metal/Acid Catalysts to Aromatic Oligomers. *Chemical Engineering Journal* **2020**, *399*, 125712. <https://doi.org/10.1016/j.cej.2020.125712>.
- (69) Anderson, E. M.; Katahira, R.; Reed, M.; Resch, M. G.; Karp, E. M.; Beckham, G. T.; Román-Leshkov, Y. Reductive Catalytic Fractionation of Corn Stover Lignin. *ACS Sustainable Chem. Eng.* **2016**, *4* (12), 6940–6950. <https://doi.org/10.1021/acssuschemeng.6b01858>.
- (70) Yuan, Z.; Tymchyshyn, M.; Xu, C. (Charles). Reductive Depolymerization of Kraft and Organosolv Lignin in Supercritical Acetone for Chemicals and Materials. *ChemCatChem* **2016**, *8* (11), 1968–1976. <https://doi.org/10.1002/cctc.201600187>.
- (71) Wang, D.; Li, G.; Zhang, C.; Wang, Z.; Li, X. Nickel Nanoparticles Inlaid in Lignin-Derived Carbon as High Effective Catalyst for Lignin Depolymerization. *Bioresource Technology* **2019**, *289*. <https://doi.org/10.1016/j.biortech.2019.121629>.
- (72) Asmadi, M.; Kawamoto, H.; Saka, S. Thermal Reactions of Guaiacol and Syringol as Lignin Model Aromatic Nuclei. *Journal of Analytical and Applied Pyrolysis* **2011**, *92* (1), 88–98. <https://doi.org/10.1016/j.jaap.2011.04.011>.
- (73) Sjöström, E. Chapter 4 - LIGNIN. In *Wood Chemistry (Second Edition)*; Sjöström, E., Ed.; Academic Press: San Diego, 1993; pp 71–89. <https://doi.org/10.1016/B978-0-08-092589-9.50008-5>.